
The quest for obscured AGN at cosmological distances: Infrared Power-Law Galaxies

Almudena Alonso-Herrero^{1,2}, Jennifer L. Donley², George H. Rieke², Jane R. Rigby^{3,2} and Pablo G. Pérez-González^{4,2}

¹ DAMIR, Instituto de Estructura de la Materia, CSIC, 28006 Madrid, Spain

² Steward Observatory, University of Arizona, Tucson, AZ 85721, USA

³ Carnegie Observatories, Pasadena, CA 91101, USA

⁴ Departamento de Astrofísica y CC de la Atmósfera, UCM, 28040 Madrid, Spain

Summary. We summarize multiwavelength properties of a sample of galaxies in the *Chandra* Deep Field North (CDF-N) and South (CDF-S) whose Spectral Energy Distributions (SEDs) exhibit the characteristic power-law behavior expected for AGN in the *Spitzer*/IRAC 3.6–8 μm bands. AGN selected this way tend to comprise the majority of high X-ray luminosity AGN, whereas AGN selected via other IRAC color-color criteria might contain more star-formation dominated galaxies. Approximately half of these IR power-law galaxies in the CDF-S are detected in deep (1 Ms) *Chandra* X-ray imaging, although in the CDF-N (2 Ms) about 77% are detected at the 3σ level. The SEDs and X-ray upper limits of the sources not detected in X-rays are consistent with those of obscured AGN, and are significantly different from those of massive star-forming galaxies. About 40% of IR power-law galaxies detected in X-rays have SEDs resembling that of an optical QSO and morphologies dominated by bright point source emission. The remaining 60% have SEDs whose UV and optical continuum are much steeper (obscured) and more extended morphologies than those detected in X-rays. Most of the IR power-law galaxies not detected in X-rays have IR (8 – 1000 μm) above $10^{12} L_{\odot}$, and X-ray (upper limits) to mid-IR ratios similar to those of local warm (ie, hosting an AGN) ULIRGs. The SED shapes of power-law galaxies are consistent with the obscured fraction (4:1) as derived from the X-ray column densities, if we assume that all the sources not detected in X-rays are heavily absorbed. IR power-law galaxies may account for between 20% and 50% of the predicted number density of mid-IR detected obscured AGN. The remaining obscured AGN probably have rest-frame SEDs dominated by stellar emission.

1 Introduction

Active Galactic Nuclei (AGN) are sources of luminous X-ray emission, and at cosmological distances AGN are routinely selected from deep X-ray (< 10 keV) exposures ([8]). Highly obscured ($N_{\text{H}} > 10^{23} - 10^{24} \text{ cm}^{-2}$) AGN are thought to be a major contributor to the hard X-ray background ([24, 9, 39, 40]). However, the majority of them might not be detected in these X-ray

surveys because a large fraction of their soft X-ray, UV, and optical emission is absorbed, and presumably reradiated in the infrared (IR).

Numerous attempts have been made to detect this population of heavily obscured AGN, many of which have focused on the MIR emission where the obscured radiation is expected to be reemitted (e.g., [4, 20, 32, 28, 11]), or on combinations of MIR and multiwavelength data (e.g., [10, 23]). In the mid-IR, AGN can often be distinguished by their characteristic power-law emission (e.g., [25, 13]). This emission is not necessarily due to a single source, but can arise from the combination of non-thermal nuclear emission and thermal emission from various nuclear dust components ([29]). We summarize here the properties of galaxies showing the characteristic power-law behavior expected for AGN in the *Spitzer* 3.6 – 8 μm bands detected in the *Chandra* Deep Field North and South (CDF-N and CDF-S) studied in [4] and [11], respectively. We also discuss results from other IR-based methods to detect high- z obscured AGN. We use $H_0 = 71 \text{ km s}^{-1} \text{ Mpc}^{-1}$, $\Omega_M = 0.3$, and $\Omega_\Lambda = 0.7$.

2 The Sample of IR power-law galaxies

2.1 Selection

We chose two cosmological fields with deep X-ray coverage (CDF-N: 2 Ms and CDF-S: 1 Ms, see [1] for details) to look for obscured AGN. We selected as power-law galaxies sources that were detected in each of the four IRAC (3.6, 4.5, 5.8, and 8 μm) bands and whose IRAC spectra could be fitted as $f_\nu \propto \nu^\alpha$, where α is the spectral index. We used a minimum χ^2 criterion to select galaxies whose IRAC SEDs followed a power law with spectral index $\alpha < -0.5$. The choice for the spectral index was based on the empirical spectral energy distributions (SEDs) of bright QSO selected in the optical, X-rays and near-IR (e.g., [25, 13, 18, 19]) and Seyfert galaxies (e.g., [36, 12]). There are two slight differences in the two catalogs of IR power-law galaxies. In the CDF-S [4] started the selection of the power-law candidates from the 24 μm catalog of [26], without any further requirements on the flux limits of the IRAC catalogs. [11] in the CDF-N instead imposed a strict S/N= 6 flux density cut in each of the IRAC bands but did not require a 24 μm detection, although virtually all of the power-law galaxies in the CDF-N were also detected at 24 μm down to $\sim 80 \mu\text{Jy}$ (equivalent to the 80% completeness limit of the CDF-S, see [26]).

To minimize the chances of selecting non-active galaxies we constructed optical-MIR SEDs (see §4), and compared them with theoretical and observational templates of star-forming galaxies. We rejected any source selected via the power-law criteria whose SED resembled a star-forming galaxy. The final samples included 92 and 62 galaxies in the CDF-S and CDF-N, respectively (see [4] and [11] for details).

A small ($\sim 25 - 30\%$, depending on the field) fraction of the power-law galaxies, typically the optically bright X-ray sources (see next section), have

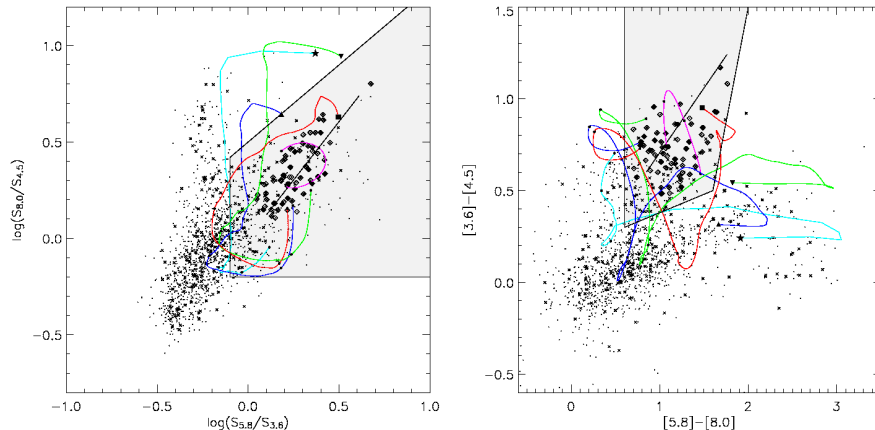


Fig. 1. Location of the CDF-N IR power-law galaxies (diamonds) on the Lacy et al. (left) and Stern et al. (right) IRAC color-color diagrams together with X-ray sources (crosses from [1]) and IRAC galaxies (dots, non power-law galaxies) detected in this field. The shaded regions indicate the AGN loci, and the straight lines within them the power-law criterion. We also show the z -evolution ($z = 0 - 2.5$ where $z = 0$ is indicated by the large symbol at the edge of each template line) of different templates. In green (upside down triangle) a starburst ULIRG, in blue (triangle) Arp 220, in red (square) an AGN ULIRG, in pink (filled dot) the average of the radio-quiet QSOs of [13], and in cyan (star symbol) a star-forming galaxy.

spectroscopic redshifts (e.g., [33] in CDF-S). We supplemented the available spectroscopic redshifts with photometric ones estimated with an improved version of the method described by [27]. We find that the IR power-law galaxies tend to lie at significantly higher redshifts ($z > 1$) than the X-ray sources (median $z \sim 0.7$, see [8] for a review) in both fields.

2.2 Comparison between IRAC power-law and color-color criteria

[20] and [32] defined AGN selection criteria based on *Spitzer*/IRAC color-color diagrams. The Lacy et al criterion is based on SDSS QSOs, and therefore excludes AGN in which the host galaxy dominates the MIR (see e.g., [3, 31, 14, 28]), as well as AGN obscured in the mid-IR. Our power-law galaxies fall along a straight line well within the Lacy et al diagram, although they do not cover completely the available color space (see Fig. 1). The Stern et al criteria are based on the observed properties of spectroscopically classified AGN, and provide a closer match to our power-law technique. While the color-color selected samples comprise a higher fraction of the low X-ray luminosity AGN than does the power-law selected sample, the color criteria select more sources not detected in X-rays, due at least in part to a higher degree of contamination from ULIRGs dominated by star formation (Fig. 1 and [6]).

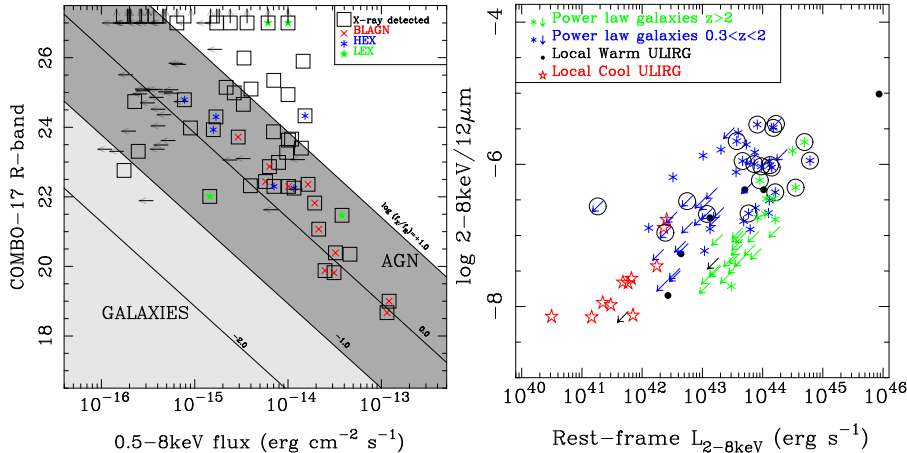


Fig. 2. *Left panel:* COMBO-17 ([38]) *R*-band versus the *Chandra* full band flux of IR power-law galaxies in the CDF-S (similar results are found for the CDF-N). When available we show the optical spectroscopic classifications from [33] (see §5 for details). The galaxies in our sample not detected by COMBO-17 are shown as upper limits at $R = 27$ mag. *Right panel:* Rest-frame 2–8 keV luminosity vs hard X-ray to 12 μ m for IR power-law galaxies (asterisks and X-ray upper limits; the circles denote those classified as BLAGN) in the CDF-S compared with local cool (no AGN) and warm (hosting an AGN) ULIRGs.

Recently [21] obtained follow-up optical spectroscopy of objects selected according to [20] in the *Spitzer* First Look Survey and SWIRE XMM-LSS fields. Their sample is flux-limited at 24 μ m, although their objects are much brighter ($f_{24\mu\text{m}} = 4 - 20$ mJy, median of 5 mJy, and median *R*-band magnitudes $R \sim 18$ mag) than our power-law galaxies ($f_{24\mu\text{m}} \sim 0.08 - 3$ mJy, and $R \sim 23$ mag for those detected by COMBO-17 see next section), and on average their AGN are closer $z_{\text{sp}} \sim 0.6$ compared with $z \sim 1.5$ for our power-law galaxies. The location of this sample on the [20] IRAC color-color diagram (figure 7 in [21]) is almost identical to the positions of the power-law galaxies shown in Fig 1 (right panel). Their selection technique has proven to be very effective at selecting AGN as their follow-up spectroscopy shows that approximately 90% have AGN signatures with one-third of them showing broad-line regions, thus an obscured-to-unobscured ratio of 2:1 (see §5 for the power-law galaxies). All these properties seem to indicate that these color-color selected galaxies represent the brightest end of the power-law galaxies.

3 X-ray, Infrared, and Optical Properties

In both CDF-N and CDF-S we found that approximately 50% of the IR power-law galaxies were detected in at least one *Chandra* band using the X-ray

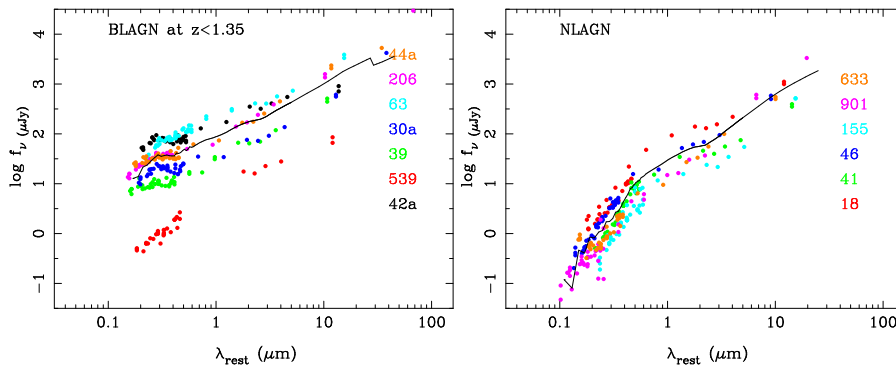


Fig. 3. Rest-frame SEDs (filled circles) of CDF-S IR power-law galaxies detected in X-rays with spectroscopic redshifts and classifications from [33] (IDs given on the right-hand side of each panel). For each SED class (only the BLAGN and NLAGN classes are shown, see [4] for more details) we have constructed an average template, shown as the solid line in each panel.

catalogs of [1]. In the CDF-S we stacked the X-ray data of a few individually undetected galaxies (at off-axis angles of $\theta < 7.5'$) and found a significant detection in the hard-band (3.1σ) and a tentative detection in the soft band (2σ). For $z = 2$ these would correspond to observed soft and hard luminosities of $< 7 \times 10^{41} \text{ erg s}^{-1}$ and $4 \times 10^{42} \text{ erg s}^{-1}$, respectively. This is consistent with obscured AGN. Since the X-ray exposure of the CDF-N is twice that of CDF-S we searched for faint X-ray emission at the positions of the power-law galaxies not in the [1] catalog. We found that the X-ray detection rate increases to 77% at the 3σ level. The power-law galaxies make up a significant fraction of the high X-ray luminosity sample, as our selection criteria require the AGN to be energetically dominant. The lower luminosity X-ray sources not identified as power-law galaxies tend to be dominated by the $1.6 \mu\text{m}$ stellar bump in the optical to near-IR bands (see also [3, 14, 28, 31]).

A large fraction of IR luminous high- z galaxies have been found to host AGN (e.g., SCUBA galaxies [2]), and IR luminous galaxies at $z \sim 1 - 2$ (e.g., [42]). We measured the total IR ($8 - 1000 \mu\text{m}$) luminosity of the CDF-S power-law galaxies from the rest-frame $12 \mu\text{m}$ luminosity. Although our procedure to compute IR luminosities is similar to that of [27], we took special care to use $12 \mu\text{m}$ to IR luminosity ratios specific to the class of galaxies in study. In particular, galaxies whose SEDs resemble those of optical QSOs (see §4 and Fig. 3) show $12 \mu\text{m}$ to IR luminosity ratios significantly lower than the typical values of cool ULIRGs and some warm ULIRGs (e.g., Mrk 231). All the IR power-law galaxies are highly luminous. About 30% are in the hyperluminous class ($L_{\text{IR}} > 10^{13} L_{\odot}$), 41% are ULIRGs ($L_{\text{IR}} = 10^{12} - 10^{13} L_{\odot}$), and all but one of the rest are LIRGs ($L_{\text{IR}} = 10^{11} - 10^{12} L_{\odot}$). At the lower IR luminosity end ($L_{\text{IR}} < 10^{12} L_{\odot}$) a large fraction are detected in X-rays and tend to have SEDs similar to those of optical QSOs (see next section).

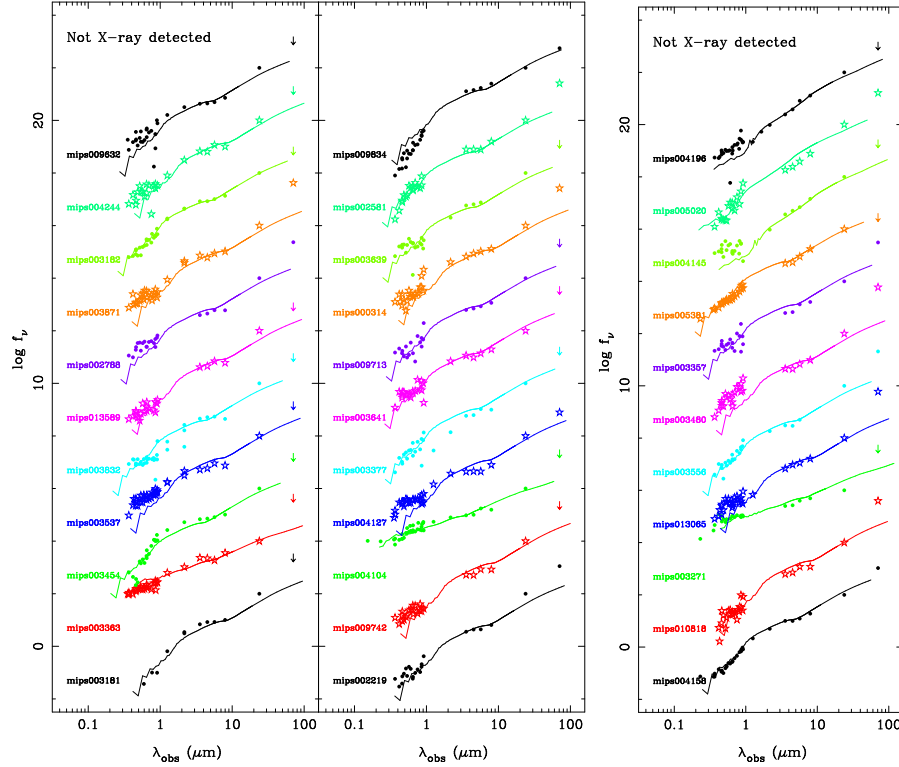


Fig. 4. Examples of the observed SEDs (filled circles and star symbols) of CDF-S IR power-law galaxies not detected in X-rays. Each galaxy is shown with the closest average template constructed using the X-ray detected ones (see [4] for details).

About one-quarter of the CDF-S IR power-law galaxies are optically faint i.e., were not detected by COMBO-17 ([38]) down to a limit of $R \sim 26.5$ mag. Moreover, the fraction of power-law galaxies not detected in X-rays increases toward fainter R -band magnitudes (see Fig. 2), an indication of their obscured nature as also revealed by their SEDs (see also §5). A number of works (e.g., [7] and references therein) have demonstrated that X-ray to optical flux ratios can be useful for distinguishing between AGN and star-forming galaxies for sources detected in deep X-ray exposures. Fig. 2 (left panel) shows that the majority of the galaxies (or their upper limits) in the CDF-S are consistent with being AGN or transition objects based on the X-ray vs. R -band diagram (similar results are found for the CDF-N galaxies). The location of the IR power-law galaxies on this diagram (see [7]) indicates X-ray luminosities (or upper limits) above 10^{41} erg s $^{-1}$, as also shown by the right panel of Fig. 2. The rest-frame hard X-ray/ $12 \mu\text{m}$ ratios of the IR power-law galaxies are similar to those of local warm ULIRGs (i.e., those containing an AGN) and QSO.

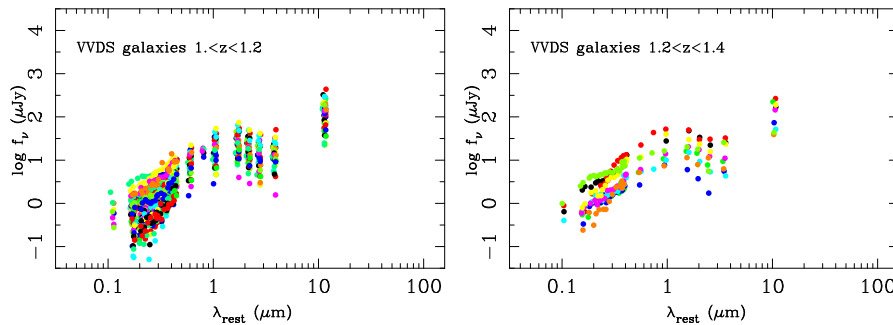


Fig. 5. Examples of rest-frame SEDs of CDF-S VVDS galaxies at $z > 1$ included in the sample of predominantly star-forming galaxies selected at $24\ \mu\text{m}$ by [27].

4 SEDs and Morphologies

Using available multiwavelength datasets (see [4, 11] for references) of the two cosmological fields we constructed SEDs for our sample. The spectroscopic classifications (broad vs. narrow lines⁵) tend to agree with two distinct types of SEDs. About 40% of the CDF-S IR power-law galaxies detected in X-rays are classified as BLAGN and have SEDs (Fig. 3) similar to the average radio-quiet QSO SED of [13], that is, with an optical-to-mid-IR continuum almost flat in νf_ν with a UV bump. The remaining X-ray sources with narrow lines (NLAGN) have SEDs similar to the BLAGN but their UV and optical continua are much steeper (obscured), and some of them resemble local warm ULIRGs. The majority of the power-law galaxies not detected in X-rays (Fig. 4) have steep SEDs similar to the NLAGN or ULIRG class as they tend to be optically fainter (see §3) and possibly more obscured (see §5) than the X-ray sources.

In contrast with our power-law galaxies, massive galaxies from the VIR-MOS VLT Deep Survey (VVDS, [22]) at $1 < z < 2$ with $24\ \mu\text{m}$ detections from the sample of [27] are predominantly star-forming galaxies with a prominent stellar bump at $1.6\ \mu\text{m}$ due to an evolved (red giants and supergiants) stellar population. Moreover, the SEDs of power-law galaxies are also significantly different from those of the majority of optically-dull AGN in the CDF-S which show SEDs dominated by stellar light originating in the host galaxy (see [31]).

Fig. 4 shows the Great Observatories Origins Deep Survey (GOODS) ACS ([15]) observed optical morphologies of optically-bright power-law galaxies in the CDF-S. The power-law galaxies spectroscopically classified as BLAGN (and SED type) display bright nuclear point sources suggesting that the optical light is dominated by the AGN, which is consistent with the fact that our

⁵ The Szokoly et al. spectral classifications of CDF-S X-ray sources with clear AGN signatures were: BLAGN (broad-line AGN) and HEX (high excitation lines). Approximately 50% of their X-ray sources did not have a clear AGN signature in their optical spectra: LEX (low excitation lines, also termed optically-dull AGN and X-BONGS) and ABS (absorption lines).

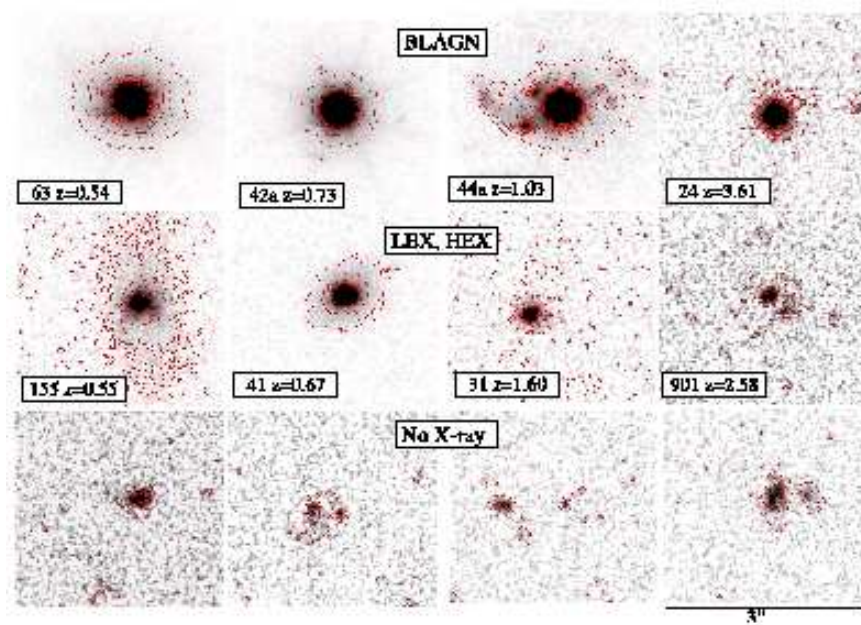


Fig. 6. Postage stamps of optically-bright power-law galaxies in the CDF-S. The data are from the public release of the GOODS *HST*/ACS F606W images. Examples of X-ray detected power-law galaxies are shown in the top and middle panels with the IDs, and spectroscopic redshifts and classifications from [33]. Power-law galaxies not detected in X-rays are shown in the bottom panel.

power-law criteria selects the most X-ray luminous AGN (see also [31]). The power-law galaxies without broad lines (those classified as HEX or LEX by [33]) have diskly or irregular morphologies. A morphological characterization of the IR power-law galaxies not detected in X-rays is difficult as only about half of them are detected in the GOODS/ACS images and they are faint. As can be seen for a few examples in Fig. 4 they have irregular, knotty, and/or interacting morphologies, and do not appear to contain bright point sources.

5 Obscuration and Obscured Fraction

In the distant universe the X-ray background and luminosity synthesis models predict global obscured ($N_{\text{H}} \geq 10^{22} \text{ cm}^{-2}$) to unobscured ratios of 3:1 to 4:1 (e.g., [9, 16]), significantly higher than the observed ratios of spectroscopically identified X-ray sources in deep fields (e.g., [5, 33]) including those detected in the mid-IR (e.g., [30]). [11] estimated the intrinsic column densities of each of the X-ray well detected and weakly X-ray emitting power-law galaxies in the

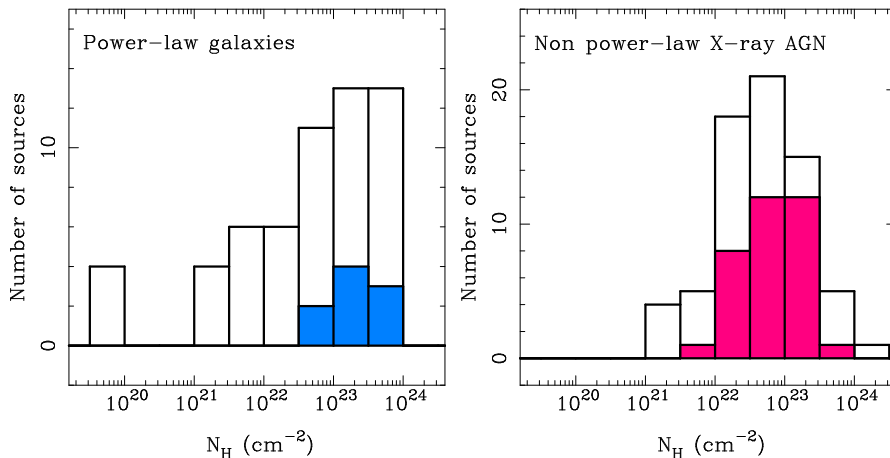


Fig. 7. *Left panel.* Distribution of X-ray column densities for the CDF-N power-law galaxies that are cataloged X-ray sources (empty) and those only weakly detected in X-rays (shaded) from [11]. We also include those CDF-S power-law galaxies selected by [4] for which [31] measured a column density. *Right Panel.* N_{H} distribution for all the CDF-S X-ray optically active AGN (empty) with spectroscopic classifications [33, 31], excluding all the power-law galaxies shown in the left panel. The shaded histogram shows the N_{H} of the optically-dull AGN (only those classified as LEX).

CDF-N. We also included a few CDF-S IR power-law galaxies ([4]) for which [31] estimated the X-ray column densities. The column density distribution of the power-law galaxies (Fig. 7) is significantly different from that of optically bright X-ray AGN with spectroscopic classifications (see also [34]), including the optically-dull AGN which are believed to suffer strong obscuration ([31]). From Fig. 7 it is clear that the weakly detected IR power-law galaxies are consistent with being obscured ($N_{\text{H}} \sim 10^{22} - 10^{24} \text{ cm}^{-2}$) but not Compton-thick ($N_{\text{H}} \geq 10^{24} \text{ cm}^{-2}$). If all the X-ray non-detected power-law galaxies are obscured, the maximum obscured ratio is 4:1 (for the CDF-N power-law galaxies). This N_{H} -based obscured fraction of power-law galaxies agrees well with the ratio of BLAGN (unobscured) SED vs. NLAGN (obscured) SEDs found in the CDF-S.

We can finally estimate the ratio of obscured to unobscured mid-IR detected AGN in the CDF-S. The unobscured AGN are all those X-ray sources (detected in the hard band to make sure they are AGN) with $N_{\text{H}} < 10^{22} \text{ cm}^{-2}$, whereas in the obscured category we include all obscured X-ray sources with $N_{\text{H}} > 10^{22} \text{ cm}^{-2}$, and all the obscured IR power-law galaxies. We find an observed ratio of obscured to unobscured AGN of 2:1 in the CDF-S. Comparing with the predictions of [35] for the $24 \mu\text{m}$ detected AGN number density we find that our sample of power-law galaxies only accounts for approximately 20% of all the mid-IR emitting obscured AGN in the CDF-N. This fraction can be as high as $\sim 50\%$ in the CDF-S as a result of larger sample of power-

law galaxies there (we did not impose IRAC high S/N detections, see §2 and [4, 11] for details). The remainder should have SEDs dominated by or strongly affected by the host galaxy or red power-law SEDs that fall below the IRAC detection limit. This is not surprising as our power-law criteria require the AGN to be energetically dominant in the near to mid-IR.

6 Other Infrared-Based Searches for Obscured AGN

The selection of IR-bright optically-faint galaxies has been suggested as another method for identifying obscured AGN ([17, 37]), although the selection criteria ($R > 23.9$ and $f_{24\mu\text{m}} > 0.75 - 1$ mJy) were set so that IRS follow-up spectroscopy could be obtained. These criteria select mostly high- z (median $z \sim 2.2$) galaxies, with only a small fraction showing the characteristic aromatic feature emission of star forming galaxies. The majority have IRS spectra similar to local AGN-dominated ULIRGs with either a featureless power-law rest-frame mid-IR continuum or deep silicate features at $9.7\mu\text{m}$. In addition, their SEDs lack a strong $1.6\mu\text{m}$ stellar bump, and are similar to those of IR power-law galaxies. Their properties are consistent with being optically obscured AGN-powered ULIRGs with $L_{\text{IR}} > 10^{12} L_{\odot}$ (see [17, 37] for details).

Only a few galaxies in the CDF-N and CDF-S fall within the [17, 37] flux density cuts. We can instead compare with the $24\mu\text{m}/8\mu\text{m}$ vs. $24\mu\text{m}/R$ -band diagram criterion proposed by [41, 42] to select obscured AGN. The location of our CDF-N power-law galaxies on this diagram can be seen in Fig. 8. We also show the comparison X-ray sources (from [1]) and other IRAC sources in the field that do not meet the power-law criteria. We find that all these samples cover a large range in colors, but the power-law galaxies comprise a significant fraction ($\sim 30 - 40\%$) of the highly optically reddened members of the comparison X-ray sample. This suggests that the power-law selection is capable of detecting both optically obscured and unobscured AGN, and that a large fraction of the IR-bright/optically-faint sources in the comparison sample have power-law SEDs in the near and mid-IR (Fig. 8).

Radio emission is another good way to select AGN as it is unaffected by dust absorption. [10] in the CDF-N used a radio to mid-IR ratio to select galaxies that are too bright in radio to be star-forming galaxies. They found that $\sim 30\%$ of their radio-loud AGN are not detected in X-rays suggesting strong obscuration. [23] looked for a population of radio intermediate and radio quiet AGN by selecting $24\mu\text{m}$ sources ($f_{24\mu\text{m}} \sim 0.3 - 1$ mJy) with radio emission and imposed a flux density cut at $3.6\mu\text{m}$ to filter out type-1 and radio-loud QSOs. They found a population of QSOs at $1.4 < z < 4.2$ (median $z = 2$, the epoch of QSO maximum activity) with a ratio of obscured to unobscured of $(2 - 3):1$, and postulated that this population of obscured AGN may be responsible for most of the black hole growth in the young universe.

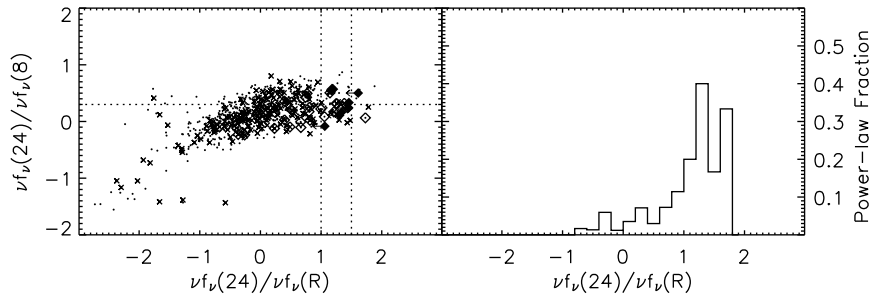


Fig. 8. Location of the CDF-N power-law galaxies and comparison samples (symbols as in Fig. 1) on the color-color diagram of [41] (left panel) where the dotted lines indicate the Yan et al. selection criteria for possible dust-reddened AGN. The right panel shows the power-law fraction of the IRAC comparison sample (non power-law galaxies) as a function of the 24 μm over R -band flux ratio.

7 Summary

Deep X-ray cosmological surveys are efficient at detecting AGN at high- z but they only account for a $\sim 1:1$ ratio of obscured-to-unobscured AGN, whereas synthesis models of the X-ray background require ratios of between 3:1 and 4:1. Thus there is a significant population of obscured ($N_{\text{H}} > 10^{23} - 10^{24} \text{ cm}^{-2}$) AGN being missed by current deep X-ray ($< 10 \text{ keV}$) observations. We describe searches for this population. Our selection criterion is based on the characteristic IR power-law emission shown by local QSOs. By selecting galaxies with power-law emission in the *Spitzer*/IRAC bands (3.6, 4.5, 5.8, and 8 μm) we avoid high- z galaxies whose SEDs are dominated by stellar emission and star formation peaking at 1.6 μm .

Only $\sim 50\%$ of IR power-law galaxies are detected in deep (1–2 Ms) X-ray exposures. This fraction increases to 75% if we include weakly detected X-ray sources at the 3σ level in the field with the deepest X-ray exposure (CDF-N). The optical (faint), IR (mostly ULIRGs and hyper luminous IR galaxies), and X-ray properties, the X-ray column densities N_{H} (moderately obscured, but not Compton-thick) and redshift ($z > 1$) distributions, and SED shapes of a large fraction (up to 80%) of IR power-law galaxies are significantly different from bright X-ray selected AGN. This may indicate that a large fraction of IR power-law galaxies are good candidates to host obscured AGN, and could account for a ratio of 2:1 of obscured-to-unobscured AGN at high- z .

Other mid-IR based criteria (e.g., [10, 17, 20, 21, 23, 32, 41, 42, 37]) are also finding populations of obscured AGN. There might be a significant overlap between populations of bright mid-IR AGN selected with all these methods, and thus a complete census of the *entire* obscured AGN population is needed to determine whether we can account for the obscured fraction of the X-ray background.

A. A. H. acknowledges support from the Spanish Plan Nacional del Espacio under grant ESP2005-01480 and P. G. P.-G. from the Spanish Programa Nacional de Astronomía y Astrofísica under grant AYA 2004-01676 and the Comunidad de Madrid ASTRID I+D project. Support for this work was also provided by NASA through Contract no. 960785 and 1256790 issued by JPL/Caltech.

References

1. D.M. Alexander et al: AJ **126**, 539 (2003)
2. D.M. Alexander et al: Nature **434**, 738 (2005)
3. A. Alonso-Herrero et al: ApJS **154**, 155 (2004)
4. A. Alonso-Herrero et al: ApJ **640**, 167 (2006)
5. A. Barger et al: AJ **126**, 632 (2003)
6. P. Barmby et al: ApJ **642**, 126 (2006)
7. F.E. Bauer et al: AJ **128**, 2048 (2004)
8. W.N. Brandt & G. Hasinger: ARA&A **43**, 827 (2005)
9. A. Comastri et al: A&A **296**, 1 (1995)
10. J.L. Donley et al: ApJ **634**, 169 (2005)
11. J.L. Donley et al: ApJ submitted (2006)
12. R.A. Edelson et al: ApJ **321**, 233 (1987)
13. M. Elvis et al: ApJS **95**, 1 (1994)
14. A. Franceschini et al: AJ **129**, 2074 (2005)
15. M. Giavalisco et al: ApJ **600**, L93 (2004)
16. R. Gilli: Advances in Space Research **34**, 2470 (2004)
17. J. Houck et al: ApJ **622**, L105 (2005)
18. Z. Ivezić et al: AJ **124**, 2364 (2002)
19. J.K. Kuraszekiewicz et al: ApJ **590**, 128 (2003)
20. M. Lacy et al: ApJS **154**, 166 (2004)
21. M. Lacy et al: ApJ in press, astro-ph/0609594 (2006)
22. O. Le Fèvre et al: A&A **428**, 1043 (2004)
23. A. Martínez-Sansigre et al: Nature **436**, 666 (2005)
24. R.F. Mushotzky et al: Nature **404**, 459 (2000)
25. G. Neugebauer et al: ApJ **230**, 79 (1979)
26. C. Papovich et al: ApJS **154**, 70 (2004)
27. P.G. Pérez-González et al: ApJ **630**, 82 (2005)
28. M.C. Polletta et al: ApJ **642**, 673 (2006)
29. G.H. Rieke & M.J. Lebofsky: ApJ **250**, 87 (1981)
30. J.R. Rigby et al: ApJS **154**, 160 (2004)
31. J.R. Rigby et al: ApJ **645**, 115 (2006)
32. D. Stern et al: ApJ **631**, 136 (2005)
33. G.D. Szokoly et al: ApJS **155**, 271 (2004)
34. P. Tozzi et al: A&A **451**, 457 (2006)
35. E. Treister et al: ApJ **616**, 123 (2004)
36. M.J. Ward et al: ApJ **315**, 74 (1987)
37. D. Weedman et al: ApJ **651**, 101 (2006)
38. C. Wolf et al: A&A **421**, 193 (2004)
39. M.A. Worsley et al: MNRAS **352**, L28 (2004)
40. M.A. Worsley et al: MNRAS **357**, 1281 (2005)
41. L. Yan et al: ApJS **154**, 60 (2004)
42. L. Yan et al: ApJ **628**, 604 (2005)